The seismic velocity distribution in the vicinity of a mine tunnel at Thabazimbi, South Africa

C. Wright [a,*], E.J. Walls [b], D. de J. Carneiro [c]

[a] *Bernard Price Institute for Geophysical Research, The University of the Witwatersrand, Johannesburg, Private Bag 3, Wits 2050, South Africa*
[b] *Department of Geophysics, The University of the Witwatersrand, Johannesburg, Private Bag 3, Wits 2050, South Africa*
[c] *Formerly CSIR Mining Technology, PO Box 91230, Auckland Park 2006, South Africa*

Abstract

Analysis of the refracted arrivals on a seismic reflection profile recorded along the wall of a tunnel at an iron mine near Thabazimbi, South Africa, shows variations in P-wave velocity in dolomite away from the de-stressed zone that vary between 4.4 and 7.2 km/s, though values greater than 5.8 km/s predominate along most of the profile. The seismic velocities at the tunnel wall, however, vary between 4.2 and 5.2 km/s. Time–depth terms are in the range from 0.1 to 0.9 ms, and yield thicknesses of the zone disturbed by the tunnel excavations of between 2 and 9 m. The very low seismic velocities away from the tunnel wall in two regions are associated with alcoves or 'cubbies' involving offsets in the wall of up to 10 m. The large variations in seismic velocity resolved over distances less than 15 m with signals of wavelength around 6–9 m are attributed to variations in the sizes and concentrations of fracture systems and cracks, and in the degree of groundwater saturation of the fracture systems. The results suggest that seismic velocity variations from reflection surveys may also assist modelling studies of the stress regime in deep mines, particularly if both P and S wave velocity variations can be determined. The seismic velocity variations inferred also show that application of refraction static corrections in the processing of 'in-mine' seismic reflection profiles is as important as in surface surveys, because of the higher frequencies of the seismic energy recorded in the deep mine environment. © 2000 Elsevier Science B.V. All rights reserved.

Keywords: Seismic reflection profile; Deep mine; P-wave velocity

1. Introduction

The use of high-resolution seismic reflection and refraction methods to assist mine development was pioneered more than 40 years ago (Schmidt, 1959), and has become more widespread in recent years now that seismic data acquisition equipment has become more portable, and both computer software and high-resolution data acquisition systems are relatively inexpensive. Seismic reflection experiments applied in both mineral exploration and mine development often seek to image weakly reflecting and geometrically complex boundaries, and for surveys conducted on the surface, accurate static corrections for both elevation changes and

---

* Corresponding author. Fax: +27-11-339-7367.
  E-mail address: 006cwrig@cosmos.wits.ac.za
(C. Wright).

the variable thickness of low velocity overburden and weathering are required to image weakly reflecting structures (Spencer et al., 1993; Wright et al., 1994). The extent to which static corrections will be important in sub-surface surveys, however, is still poorly known. Furthermore, to extract the maximum amount of geological information from reflection surveys, it is preferable to use the refracted arrivals not only to provide static corrections, but to constrain geological interpretation between the survey surface and the shallowest reflectors (Wright et al., 1994; Wright, 1996).

The main objective of this paper is to provide a detailed analysis of the refracted arrivals recorded during a high-resolution seismic reflection survey in a mine tunnel at Thabazimbi, South Africa, to show that large variations in seismic velocity are created when a mine tunnel is excavated. These variations are probably due to disturbance of the ambient stress field and consequent de-stressing of the rock volume near the tunnel and small changes in temperature, resulting in the opening of cracks and fractures

within a few metres of the tunnel. The possible use of the seismic velocity variations inferred from such surveys to identify zones of weakness and to assist in quantifying local stress inhomogeneities is also examined.

2. Geology of the Thabazimbi mine

Production of iron ore in the Thabazimbi area started in 1934, and the area was the leading producer of iron in South Africa for the next quarter of a century. Ore is extracted from the banded ironstone of the Penge Formation, which overlies a band of shale of thickness varying from 2 to 10 m. Below the shale is the Frisco Formation of the Malmani dolmites (Figs. 1 and 2). A marker band of chert occurs near the top of the Frisco Formation with solution of the overlying dolomite. This has caused collapse of the overlying Penge Formation resulting in brecciation of the iron formations (Van Deventer et al., 1986).
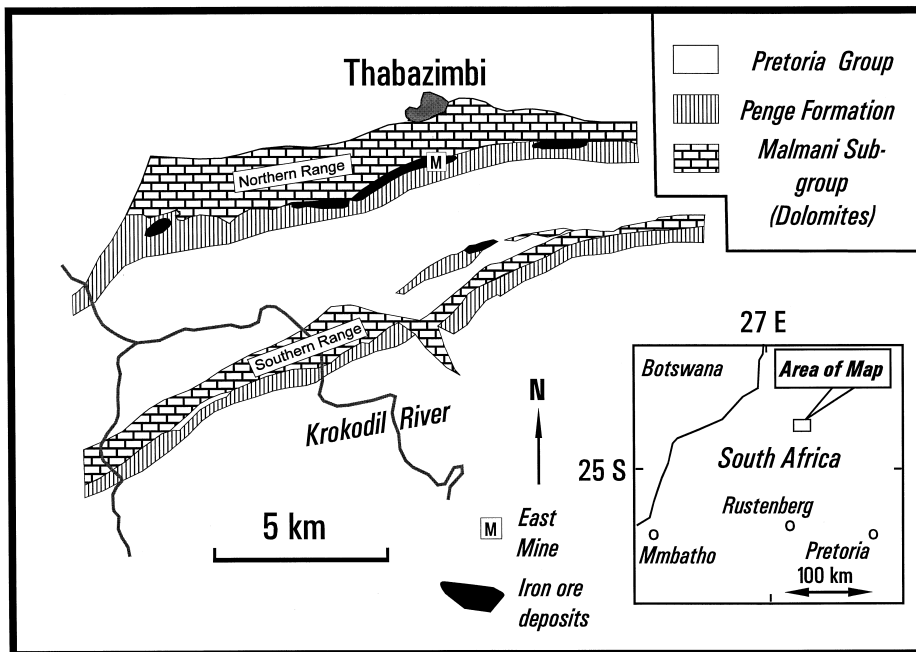

Fig. 1. Geological sketch map of the Thabazimbi mining area (adapted from Van Deventer et al. (1986)).

Fig. 2. Stratigraphy of the Proterozoic Chuniespoort Group, Western Transvaal Sequence (adapted from Van Deventer et al. (1986)).

The seismic reflection profile was undertaken in a footwall drive through the dolomite of the Frisco Formation. Fig. 3 is a vertical section showing the location of the tunnel in the dolomite, and the overlying and southerly dipping band of shale and Penge Formation. An important problem in development of the mine is the construction of a crosscut from the tunnel through the dolomite to the iron formation. To construct such a crosscut, prior knowledge of the physical properties of the intervening dolomite is required. Wad exists within the

dolomite (Fig. 3), which consists of soft, clayey manganese oxide, where the dolomite has been dissolved and altered by percolating fluids. If wad were encountered during excavations, the tunnel would be weak and likely to collapse. The contact between wad and dolomite is sharp, so that wad cavities are expected to have impedance contrasts sufficient to generate observable reflections. No wad was encountered in the walls of the mine tunnel.

3. The seismic experiment

The seismic survey was conducted during April 1997 by CSIR Mining Technology in the wall of a near-horizontal tunnel excavated in rocks of the Frisco Formation at a depth of 910 m below the surface in an iron mine (East Mine of Fig. 1) owned by Iscor Mining. The detection of zones of wad was the primary objective of the seismic study, so that a suitable position of a crosscut could be chosen. The geometry of the mine tunnel relative to the wad (Fig. 3) is such that reflected or scattered energy from the
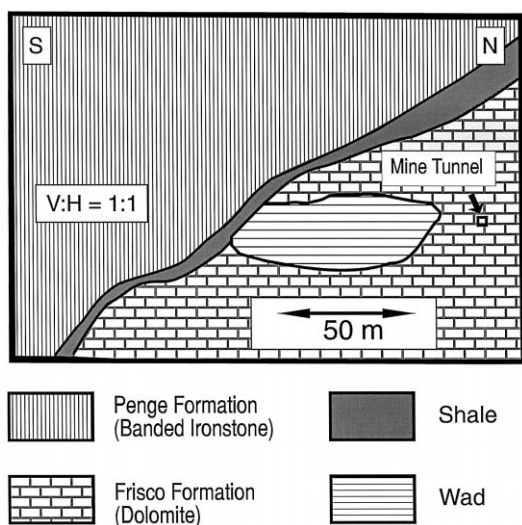

Fig. 3. Vertical section through the mine tunnel at Thabazimbi, showing the geological setting and location of targets to be imaged by seismic reflection.

Table 1
Parameters of Thabazimbi Seismic Survey, April 1997

No. of usable shots	217
Shot type, size and spacing	Explosive charges of 50 g, 1 m apart
Depth of shot holes	0.5–1.0 m
Shot-receiver configuration	Off-end (Fig. 4)
No. of geophone locations	281
Receiver spread	48 channels, takeouts 1 m apart
Geophones	Vertical component, one 100-Hz geophone per takeout mounted sideways in tunnel wall
Sampling rate	0.1 ms
Record length	100 ms
Data fold	Variable — average of 24

Shot-Receiver Configuration, Thabazimbi Mine Experiment
(not to scale)

Shot Locations 1-12   Receiver Locations 13-60

First 12 Shots

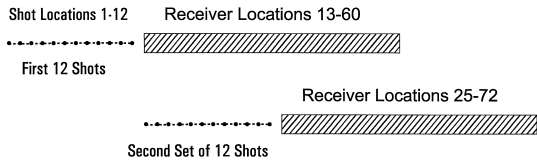Receiver Locations 25-72

Second Set of 12 Shots

Fig. 4. Shot-receiver configuration used for the seismic reflection experiment.

dolomite-wad and possibly the wad-shale boundary should be detectable. A Bison 48-channel data acquisition system was used with 100 Hz vertical-component geophones secured horizontally into the vertical mine wall (Table 1). The geophones were placed 1-m apart approximately 1.3 m above the floor of the tunnel. Seismic sources were 50 g of explosive placed in holes 0.5–1.0-m deep drilled horizontally into the wall of the tunnel at 1-m intervals at roughly the same height as the geophones. The source locations were midway between the geophones.

The shot-receiver configuration is shown in Fig. 4, and gives rise to 24-fold coverage for CMP gathers at most geophone locations. This off-end arrangement with 12 shots per location of the receiver spread was used because of the logistic difficulties in working in a mine, and the need to have sufficiently large shot-receiver offsets for velocity analysis. Two hundred seventeen usable shot records were obtained with geophone spreads covering a distance along the tunnel of 270 m (Fig. 5). The fieldwork was conducted from east to west. In displaying the results, west is always shown on the left of the diagrams. However, to illustrate methods of data analysis, the usual convention has been adopted of plotting with the start and end of the profile on the left and right, respectively.

First-break times were picked for all shots to determine both static corrections and the seismic velocity structure adjacent to the mine tunnel. Diffraction effects due to geophones in positions in which there is no straight-line shot-receiver path within the dolomite (due to the alcoves) present a problem in designing an ap-
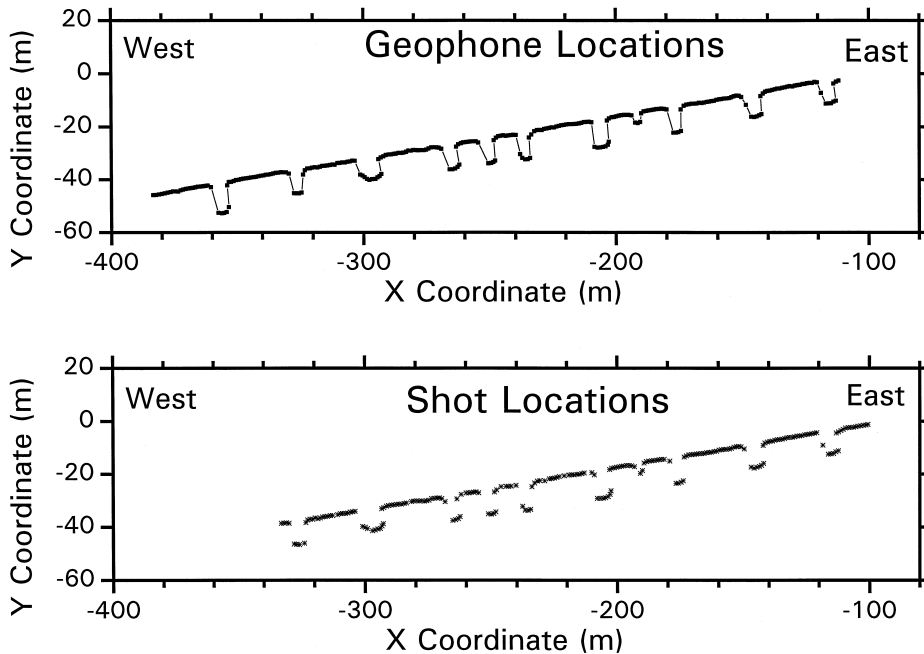
Fig. 5. Diagram showing shots and geophones in a horizontal plan.

Method of Projecting Shots and Geophones
on to a Reference Line

Projected Shot-Geophone Offset = L cos θ
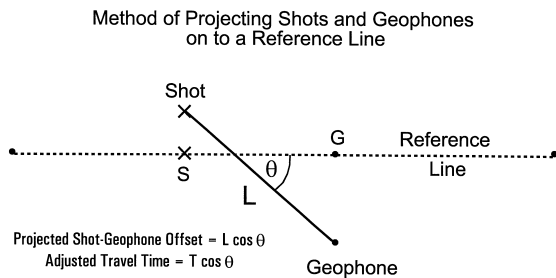Adjusted Travel Time = T cos θ

Fig. 6. Method of projecting shot and geophone locations on to a reference line defined by the first shot location and last geophone location of the profile.

propriate method of data analysis. In rare instances of extreme diffraction effects that were evident in the first-break times for some geophone locations, data were eliminated from the current analysis, which uses geometrical ray theory. For the travel-time analysis, the shot and geophone locations were projected on to a reference line joining the first shot and the most distant receiver (Fig. 6). If the angle between the line of length L joining the shot and receiver and the projected shot-receiver line SG is θ, each measured distance L and time t are replaced by corrected distances and times $L\cos\theta$ and $t\cos\theta$, respectively, for all subsequent analyses, except the estimates of seismic velocities close to the tunnel wall, for which true shot-receiver distances were used.

The mine tunnel was in a location where sources or receivers could not be placed in another tunnel or on the surface, so that the intervening rock mass could not be imaged by tunnel-to-tunnel or surface-to-tunnel tomography. The present methodology is therefore advantageous in situations where such an approach cannot be used.

4. Method of data analysis

The seismic refraction methods used in mineral exploration have usually been the reciprocal or plus–minus method (Hagedoorn, 1959; Hawkins, 1961, Hawkins and Whiteley, 1981)

or the generalized reciprocal method (Palmer, 1981), though an alternative approach involving generalized linear inversion has been tried (Hampson and Russell, 1984; De Armorim et al., 1987; Leslie, 1995). Recent modifications of the reciprocal and generalized reciprocal methods (Palmer, 1990) have not considered the important problem of how to analyse real data sets in which errors in time measurements are significant, making interpretation very subjective. In this paper a new method of applying numerical and statistical methods to optimize the resolution of lateral variations in seismic refraction velocities has been used, in which the computations are faster than when generalized linear inversion (or tomography) are used (Wright, 1999a).

4.1. Shot delay times

While measuring first-break times for estimation of shot and receiver static corrections, it became clear that the measured travel times to those geophones close to the shot point were often anomalously small (Fig. 7). The explanation is the presence of spurious and unpre-

Thabazimbi Shot Records
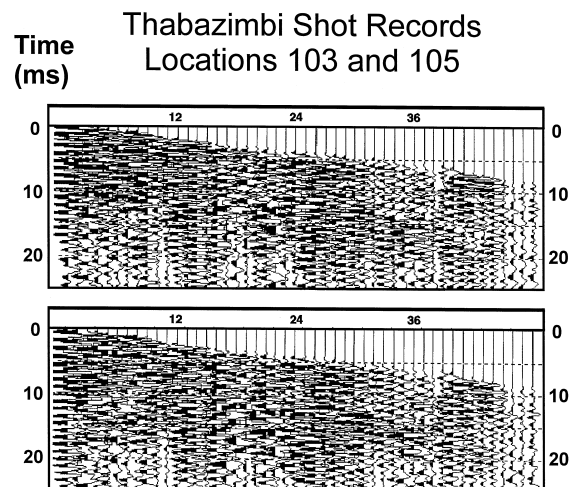Locations 103 and 105

Time (ms)

Fig. 7. Some specimen seismograms showing time delays in triggering the recording system. Estimated (minimum) delays for shots at locations 103 (top) and 105 (bottom) are 1.28 and 1.60 ms, respectively.

dictable time delays in triggering the recording system. Accurate estimates of these time delays are essential for the successful processing of the reflection data, and must be undertaken prior to the analysis of refracted arrivals to assist structural interpretation and the computation of the static corrections to be included in the reflection processing. The two shot records shown in Fig. 7 show that the recording system triggered after the earliest refracted arrivals had reached some of the geophones close to the shot point. To further illustrate the shot-timing problem, two receiver gathers are shown for locations 151 and 158 (Fig. 8), which are 4 and 11 receiver locations, respectively, from the closest shot at location 147. Both sets of receiver gathers show

Fig. 9. Method of determining relative shot delay times.

similar patterns of time variations in the first breaks due to two causes: shot-timing errors, which tend to predominate, and the locations of and conditions surrounding the shot points.

A least-squares inversion procedure has been devised for estimating these shot time delays from the first-break picks. The procedure involves fitting a least-squares line through the times for each shot gather that correspond to refracted paths in which energy has travelled beyond the low-velocity tunnel wall. Then, for each shot, time residuals are estimated for all shot gathers that are recorded by two or more geophones that lie within the distance range over which the least-squares line was calculated. The time residuals are defined as the differences between the measured times and the times determined from the line fitted through the times for the reference shot at the same shot-receiver offset (Fig. 9). The residuals are then averaged to give an estimate of the relative time delays between the shots. The procedure is repeated for all shots, and estimates of the relative time delays are optimised by a least-squares inversion procedure (Wright, 1999b).

The assumption in this method is that lateral variations in seismic velocities can be neglected for the region of the profile used in the calculations. To ensure that the assumption of lateral homogeneity for the region covered by the inversion was approximately true, the seismic profile of 217 shots was divided into 18 overlapping regions of 72 geophone locations and
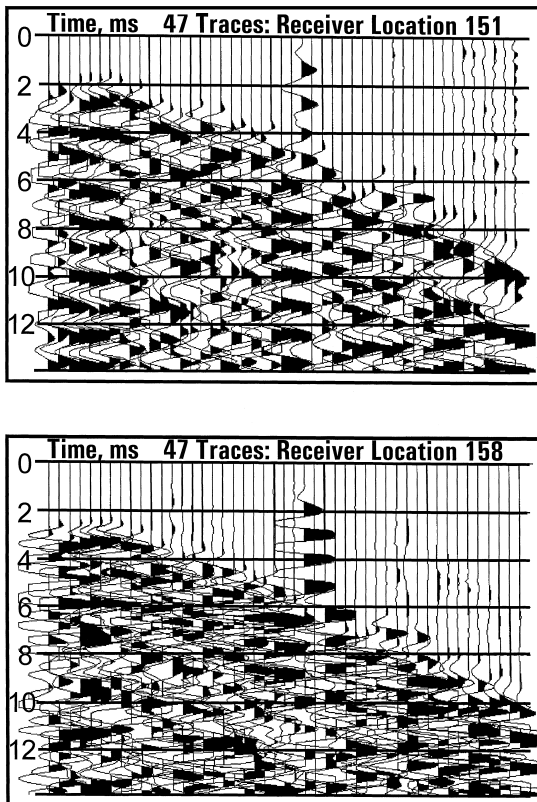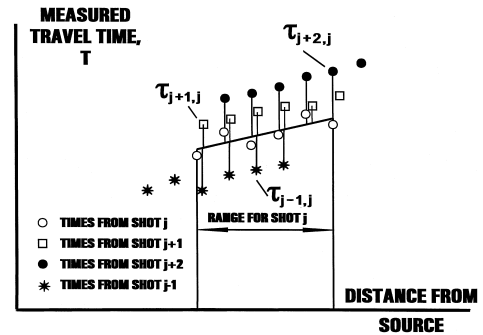

Fig. 8. Receiver gathers of locations 151 and 158, with the nearest shot at location 147 (left) and the most distant at 101 (right). The early signal at location 122 corresponds to the shot delay of 6.3 ms in Fig. 10. Note that there was no shot recorded at the location (121) of the zero trace.
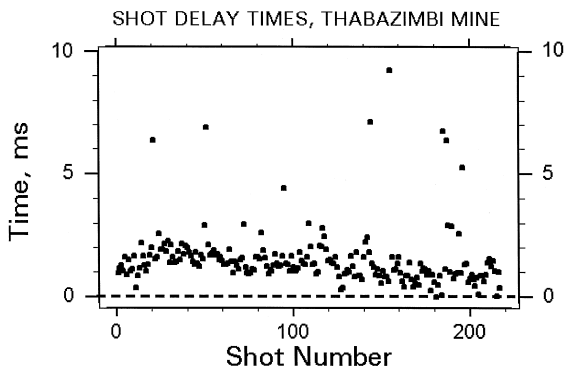
Fig. 10. Relative time delays for shots with minimum value set to zero.

30–36 shots with about two-thirds overlap between adjacent data sets, and a separate inversion for relative delay times was undertaken for each region. In instances when a shot had many missing first-break times due to large delays in triggering of the recording system, a damped least-squares procedure (Lines and Treitel, 1984) was required with several iterations to ensure convergence to a solution with low estimated variances. The results of the separate inversions were pieced together by a weighted averaging scheme. The overall solution is non-unique because an arbitrary constant can be added to all relative time delays without affecting the validity of the solution. The smallest time delay was set to zero, which corresponds to triggering of the recording system at or close to the initiation time of the seismic energy. This should give the minimum time delays required to align the shot gathers properly for further processing, though it is possible to 'overcorrect' the data if some time picks were made systematically early. We thus assume that there is just one shot for which there is no delay or a very small delay in triggering.

Fig. 10 shows the relative shot delays plotted as a function of shot number. About two-thirds of the time delays lie between 0.7 and 1.8 ms (7 and 18 samples), and there are several outliers corresponding to delays of between 4 and 10 ms. Because of the high frequencies of the

recorded seismic data (significant energy at 1 kHz), static corrections need to be determined with errors of no more than 0.3 ms. The procedure for estimating relative shot time delays allows such accuracy to be achieved.

4.2. Time–depth terms, near-surface velocities and thickness of the de-stressed layer

The reciprocal method (Hawkins, 1961) was used to estimate the time–depth terms that allow estimates of the thicknesses of the de-stressed layer (Fig. 11). Suppose a shot at A is recorded by geophones placed at B and C, and a shot at C is recorded by geophones at A and B; A, B and C lie in the same vertical plane. If the vertical velocity gradients in the lower medium are small, the time–depth is given by

$$2t_D = t_{AB} + t_{CB} - 1/2(t_{AC} + t_{CA}), \qquad (1)$$

where the t's denote times. If reversed shot-receiver paths are not available so that one of the terms of Eq. (1) is missing (t_{CA} say), we can rewrite Eq. (1) as

$$2t_D = t_{AB} + t_{CB} - t_{AC}. \qquad (2)$$

In this situation, the shot at A may be well off the end of the recording spread, so that care must be taken to ensure that velocity gradients orthogonal to the survey surface do not result in
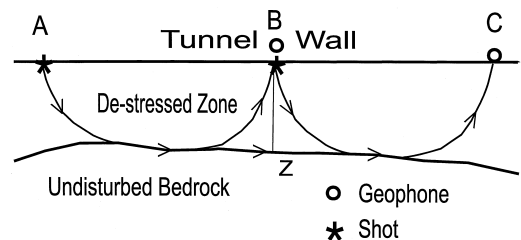

Fig. 11. Principle of the reciprocal method, when all shots are on one side of the recording spread locations. t_v is the time taken to travel the path BZ.

systematic differences in t_D as the offset AC becomes larger. Since such velocity gradients occur in most survey areas, this situation is generally unavoidable. In the present experiment, however, all shots were on one side of the recording spread, so that equivalence of time–depth terms at adjacent shot and receiver locations must be assumed for the reciprocal method to be applicable.

Seismic velocity increases gradually away from a mine tunnel. A linear increase in seismic velocity with increasing distance away from the tunnel wall was assumed and used to derive a relationship between t_D and the near-vertical travel time from the layer to the boundary, t_v. If V_1 and V_2 are the P-wave velocities at the tunnel wall and at the base of the de-stressed zone (the region affected by the tunnel excavation), the near-vertical travel time, t_v, to depth z_0 (Fig. 12) is given by

$$t_v = K^{-1}\ln(V_2/V_1), \tag{3}$$

where $V_2 = V_1 + Kz_0$, where K is a constant, so that

$$z_0 = (V_2 - V_1)/K. \tag{4}$$

Eliminating K between Eqs. (3) and (4)

$$z_0 = (V_2 - V_1)t_v/\ln(V_2/V_1). \tag{5}$$

In Fig. 12,

$$t_D = t_{D1} - t_{D2}. \tag{6}$$

From the expressions for travel times and distances for rays propagating in a medium in which velocity varies linearly with depth (Kleyn, 1983, pp. 57–58), it is shown that

$$t_{D1} = K^{-1}\ln\left(V_1/\left\{V_2 - \left(V_2^2 - V_1^2\right)^{1/2}\right\}\right) \tag{7}$$

and, if $X = $ AC in Fig. 12,

$$t_{D2} = X/V_2 = K^{-1}\left(V_2^2 - V_1^2\right)^{1/2}/V_2. \tag{8}$$

Using (Eqs. (3), (7) and (8),

$$t_D = t_{D1} - t_{D2} = C_f t_v, \tag{9}$$

where

$$C_f = \left[\ln\left(V_1/\left\{V_2 - \left(V_2^2 - V_1^2\right)^{1/2}\right\}\right)\right.$$
$$\left. - \left(V_2^2 - V_1^2\right)^{1/2}/V_2\right]/\ln(V_2/V_1). \tag{10}$$

Then,

$$z_0 = (V_2 - V_1)t_D/C_f\ln(V_2/V_1)$$
$$= (V_2 - V_1)t_D/\left[\ln\left(V_1/\left\{V_2 - \left(V_2^2 - V_1^2\right)^{1/2}\right\}\right)\right.$$
$$\left. - \left(V_2^2 - V_1^2\right)^{1/2}/V_2\right]. \tag{11}$$

We are not sure that the measured times are absolute; the times corrected for late triggering of the recording system are not necessarily close to the instant of initiation of the seismic energy. The near-surface velocities must therefore be determined by numerical differentiation of the times at short distances. All times at true distances less than 10 m, corrected for relative shot-timing errors, were used in the analysis. For each location of the receiver spread, data were arranged in increasing order of shot-receiver distance, and velocities for different distance windows were estimated for window lengths of about 5 m. In instances when there was a decrease in velocity with increasing off-
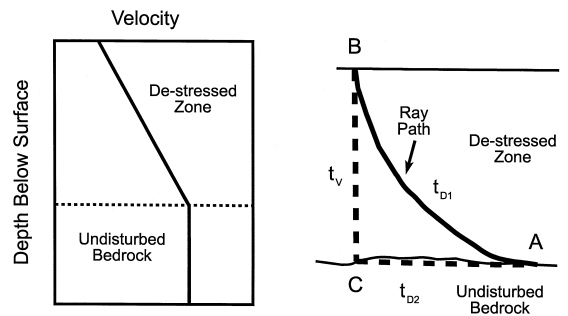

Fig. 12. Diagram showing linear variation of velocity with depth and way of estimating time-depth terms. t_v is the time taken for seismic energy to travel path BC. t_{D1} and t_{D2} are the times taken to traverse the ray path AB and the near-horizontal path AC, respectively. The time-depth t_D = $t_{D1} - t_{D2}$.
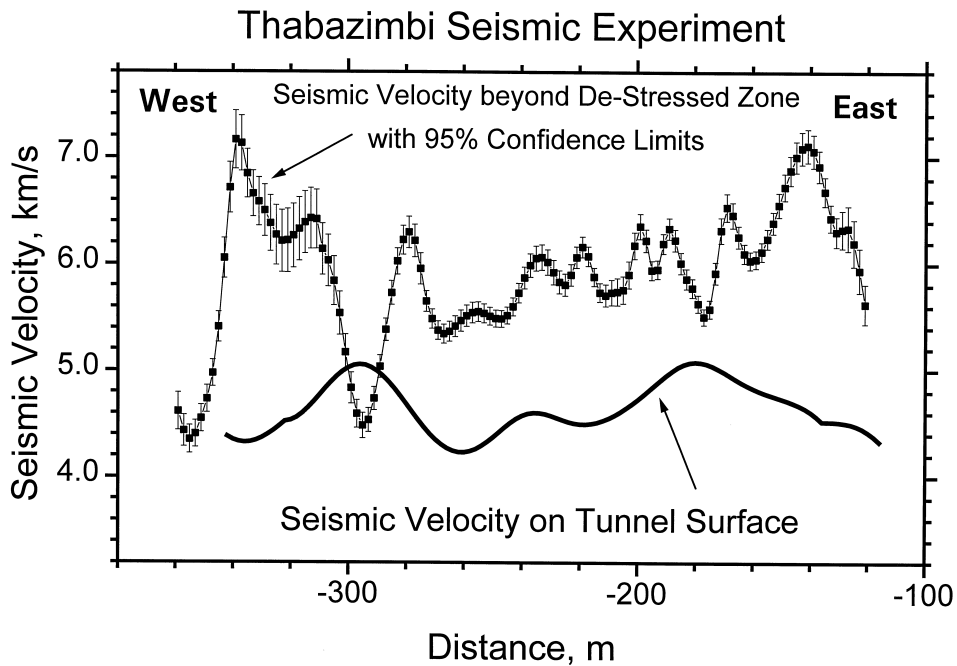
Thabazimbi Seismic Experiment

Fig. 13. P-wave velocity profile in the undisturbed zone away from the tunnel wall with 95% confidence limits on the solution, and the less accurate velocity profile for the region near the surface of the tunnel wall.

set, due to inadequate resolution, the window length was increased until the velocities increased monotonically with increasing distance. This method tends to give an upper bound to the surface velocities, and may therefore overestimate the shallow velocities by a small amount. The scattered results were then smoothed, first by the method of summary values (Jeffreys,
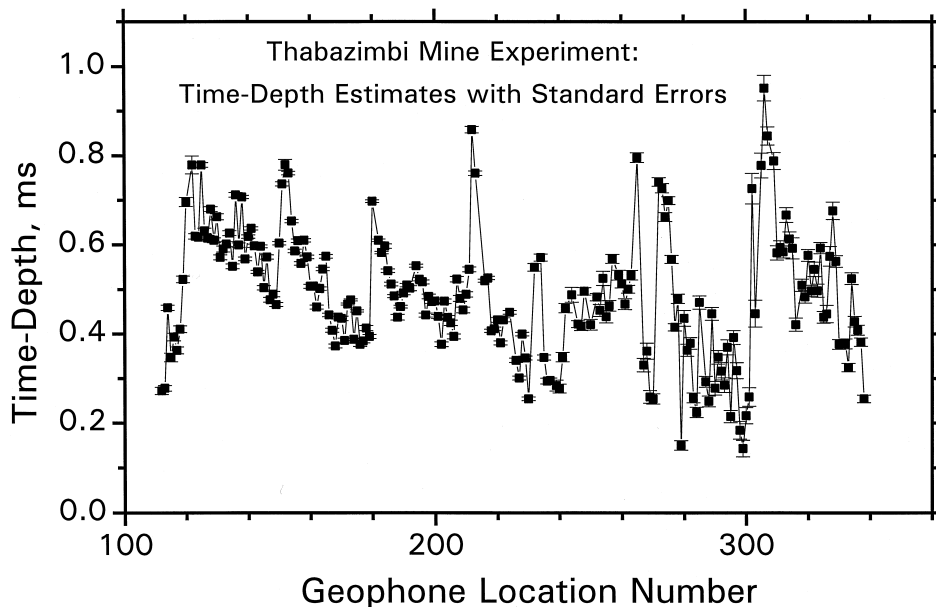
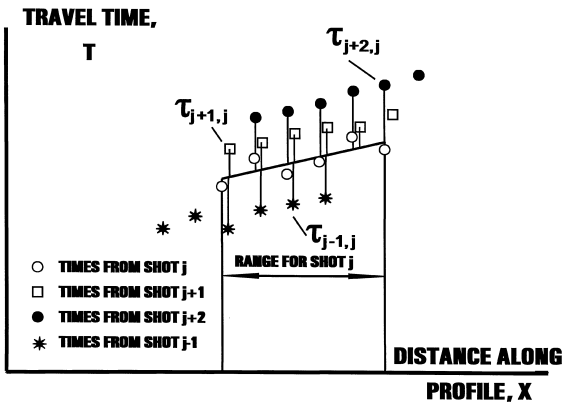Fig. 14. Time–depth terms as a function of receiver location.

Fig. 15. Method of adjusting shot times to correspond to a single shot placed on the surface of an underlying refractor.

1937; Bolt, 1978), then by a cubic spline, and then further smoothed using a 21-point sliding average to give the velocity profile shown in Fig. 13, in which the variation in velocity is from 4.2 to 5.1 km/s.

After correcting all measured times for errors in shot timing, the data were sorted into common receiver gathers. This enables time–depth terms (Fig. 12) to be derived using the reciprocity principle in which interchangeability of shots and receivers is assumed. A search over all shot and receiver gathers for which the shot-receiver offset exceeded 4.0 m was used to determine the time–depth terms at locations away from the ends of the profile, assuming that shots and receivers at the same location number have the same time–depth term. These values vary between 0.1 and 0.9 ms and are plotted in Fig. 14, and the number of time–depth terms at each location varies between 14 and 660.

4.3. Seismic velocity variations away from tunnel wall

Seismic velocity variations away from the tunnel wall were determined using the method of Wright (1999a). The time–depth terms for the shot and receiver were subtracted from each measured time to project the shots and receivers down below the de-stressed zone. A least-squares line was then fitted through the times

for each shot gather. Average residuals relative to all other shot gathers that have times measured for at least two of the same geophones as the reference shot were then calculated (Fig. 15). The set of relative corrections was optimized in a least-squares sense and applied to each shot gather to give a single travel time-versus-distance relationship corresponding to a hypothetical shot at one end of the profile (Fig. 16). To ensure convergence, data were divided into several overlapping ranges, and the separate inversions were pieced together. In most instances, a damped least-squares procedure was required, and convergence was slower when shots with many times missing were used. The construction of a single travel-time curve allows flexibility in the choice of distance windows for estimating variations in seismic velocity, and thus ensures effective use of the data (Wright, 1999a).

The method of summary values (Jeffreys, 1937; Bolt, 1978) was used to estimate seismic velocities (V_2 of Eq. (11)) in distance windows of between 14 and 26 m, with 200–600 points in each window. These windows were chosen to give errors in velocity of 0.7–3.3%, with smaller and larger errors corresponding to regions of relatively homogeneous and widely scattered data respectively. A cubic spline involving a small amount of smoothing was then fitted through the velocities to give values at intervals
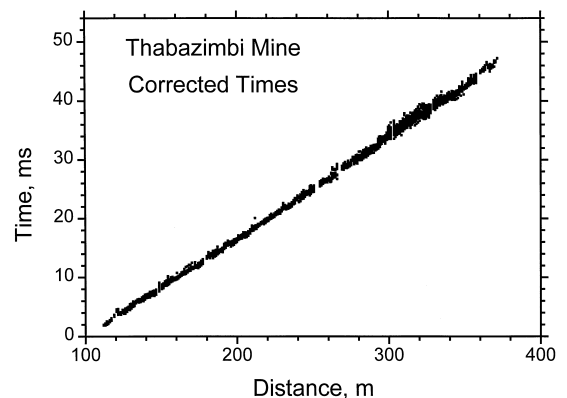

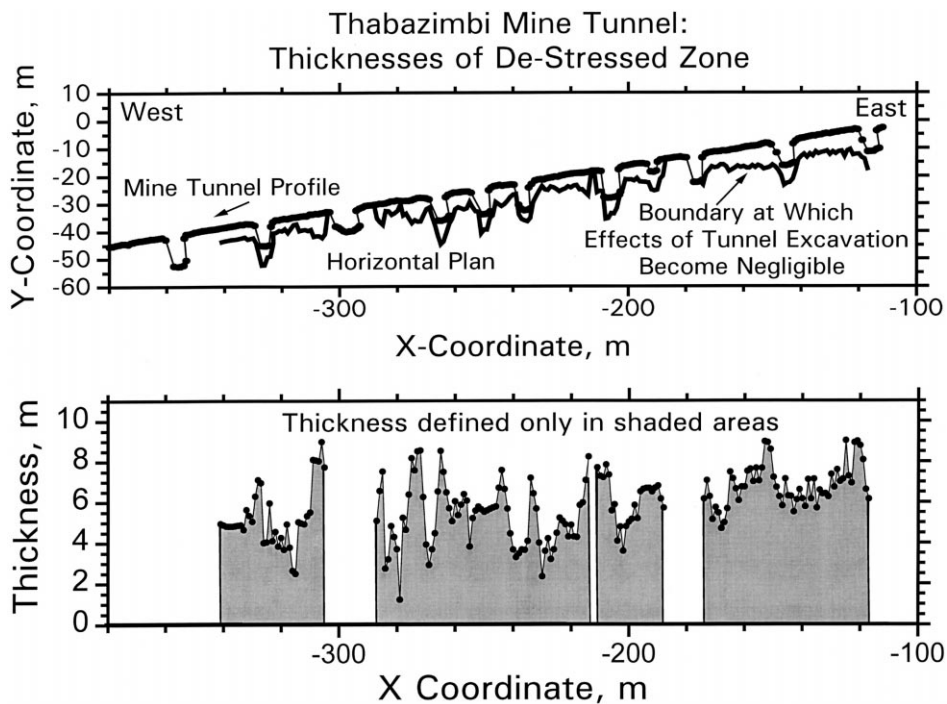Fig. 16. Corrected travel times plotted as a function of offset.

Fig. 17. Horizontal plan of mine tunnel showing approximate boundary of de-stressed zone (top), and thicknesses of the de-stressed region adjacent to the tunnel wall, as determined from Eq. (11).

of 2 m (Fig. 13). At each geophone location, an estimate of the thickness of the de-stressed zone was calculated using Eq. (11) to give the results of Fig. 17.

5. Seismic results and their interpretation

Fig. 13 shows the smoothed seismic velocities for both the surface of the mine tunnel and the region away from the tunnel excavation. There is a rough parallelism between the two curves, except that the faster seismic velocity profile for undisturbed rock exhibits greater resolution of lateral variations, because of the large number of separate time measurements (9512). There are three regions between distances of −175 and −185 m, −280 and −310 m, and from −340 to −360 m, where the seismic velocities in undisturbed rock are low compared with the estimated values on the tunnel surface. The first small local minimum is for a region

behind an alcove (Fig. 17), where the term 'behind' is used to signify the direction in which the survey was recorded, with all shots to the east of the geophone spread. The two large minima in seismic velocity between −280 and −310 m, and −340 and −360 m, cover the region both in front of and behind an alcove, making it unlikely that the velocity anomaly is a consequence of not having properly accounted for diffraction effects around the alcove walls. The very low seismic velocities suggest that these two regions are zones of weakness or high concentrations of dry fractures (see Section 6), or involve voids or potholes not far from the tunnel wall.

The velocities of Fig. 13 were used to determine the thickness of the disturbed zone using Eq. (11). The three gaps in the data are due to either absence of one or both velocities for input into Eq. (11), or very small differences between V_1 and V_2. If the difference between V_1 and V_2 is small, it seems likely that fracturing or voids

in the dolomite persist to considerable distances from the tunnel wall. On the other hand, substitution into Eq. (11) will yield very large thicknesses for the de-stressed zone for moderate-sized time–depth terms. Clearly, use of Eq. (11) is only warranted if there is a velocity increase across the de-stressed zone of at least 0.8 km/s.

While estimates of the thickness of the disturbed zone are widely scattered, there is a trend from values of 7–8 m around the −110 m position towards lower values, reaching minimum values close to 4 m between −230 and −290 m, followed by a slight upward trend to about 5 m when the *X*-coordinate is near −340 m.

6. Discussion

Rocks within the uppermost few kilometres of the earth's crust contain fractures that may be randomly distributed, or oriented in particular planes due to local or regional stress fields, resulting in seismic anisotropy. These cracks cause the seismic velocities to be lower than for a crack-free material, the amount of lowering depending on both the density of cracks and whether the cracks are dry or contain water. Overburden pressure will close cracks, resulting in an increase in seismic velocity for a particular rock type with increasing depth. A deep mine tunnel results in a change in the local stress regime, with lowering of the seismic velocities close to the tunnel walls, due to both opening of existing cracks, and the formation of new cracks during the tunnel excavation process.

The theories for seismic wave propagation in isotropic and anisotropic distributions of cracks in rocks have been reviewed by Hudson (1981) and Crampin (1981), respectively. It seems reasonable to use variations in seismic velocity in a particular rock type to infer crack properties. In Fig. 13, the maximum measured velocity of 7.2 km/s is assumed, for illustrative purposes, to approximate the conditions of a crack-free

dolomitic rock mass. This value was used to calculate the seismic velocities and Poisson's ratio as a function of crack density parameter, for both dry cracks and cracks filled with a viscous fluid, assuming an intrinsic Poisson's ratio of 0.25. The results shown in Fig. 18 were derived using the isotropic theory of O'Connell and Budiansky (1977) with the modifications suggested by Henyey and Pomphrey (1982).

The predicted velocity variations, compared with those in Fig. 13, suggest that the measured variations in P-wave velocity can only be explained if the cracks in some areas are dry or partially saturated, because they are too large to be explained in terms of water-saturated cracks at moderate crack densities. If shear-wave velocities were also measured, better constraints on the fluid content of zones of fractures and fracture density would be provided. However, the present experiment did not provide shear-wave arrivals of sufficient clarity to enable such an analysis to be undertaken. The significance of the crack density parameter (Fig. 18) is that it can be related to the actual distribution of cracks if independent information on the spectrum of crack sizes or areas can be obtained. Since seismic velocities and the distribution of cracks are also related to the stress regime, future
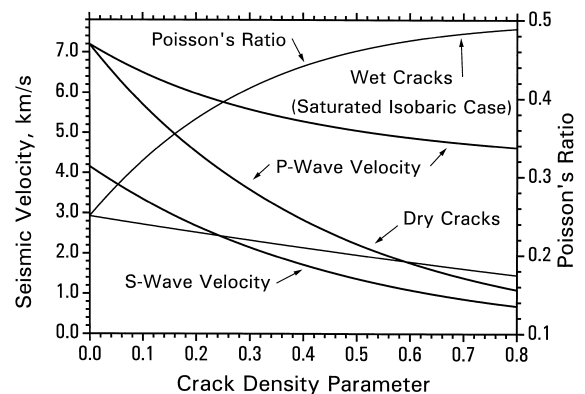

Fig. 18. Seismic velocity variations and Poisson's ratio as a function of crack density parameter for dry and saturated cracks. The results were computed using the self-consistent theory of O'Connell and Budiansky (1977), with the modifications proposed by Henyey and Pomphrey (1982).

modelling studies of the stresses in mine velocity variations.

The setting up of a seismic survey in a tunnel involves drilling into the wall to install geophones and shot locations. Both the drilling and the detonation of explosives will result in the formation of new cracks. However, the new cracks should extend only for distances of a metre or so from the geophones or shot points. The effects of both drilling and the explosive charges used in the experiment on local fracturing would be only a small addition to those already produced in excavating the tunnel. We therefore assume, to a first approximation, that the influence of the seismic experiment on the crack distribution is of secondary importance, although additional experiments would be required to confirm this.

The seismic signals have dominant frequencies of around 750 Hz, indicating wavelengths in the range 6–9 m, so that velocity variations over a distance range of 3–4 m should be detectable with high-quality data. Knowledge of these velocity variations is required to enable reliable static corrections to be derived for reflection processing, especially the contribution from 'topographic variations' associated with the 'cubbies' or alcoves (up to 2.3-ms differences between nearby shot or receiver locations). However, allowing for variations in seismic velocity both along and orthogonal to the tunnel wall is equally important, since they produce short-wavelength variations of up to 0.7 ms. Any reflected signals will have periods of about 1.3 ms, so that accurate static corrections must be applied if any reflected energy is to be enhanced through stacking.

The method of correcting for shot-timing errors will also tend to remove differences in time–depth terms between shots. Adverse consequences arise from the need to use receiver gathers to define time–depth terms, and therefore to assume that adjacent shots and receivers have the same time–depth terms. The result will be some smoothing of the differences between time–depth terms. However, if relative shot-timing errors had not been estimated, the data would have been uninterpretable. We note that this problem does not arise for split-spread recording or if shots are detonated at or near both ends of the recording spread.

7. Conclusions

Recorded seismic signals from small explosive charges in a mine tunnel about 900 m below the surface have dominant frequencies of around 750 Hz. These frequencies are very high compared with signals recorded on the surface from similar sources in tamped holes at the Earth's surface, which usually have dominant frequencies of less than 200 Hz. Better resolution of reflectors and scatterers of seismic energy away from the mine tunnel is therefore anticipated compared with surveys on the surface, but accurate refraction static corrections obtained through careful analysis of refracted arrivals must be applied during processing.

P-wave velocities in dolomite away from the de-stressed zone vary between 4.4 and 7.2 km/s, though values greater than 5.8 km/s predominate along most of the profile. The seismic velocities at the tunnel wall, however, vary between 4.2 and 5.2 km/s. Estimated thicknesses of the zone disturbed by the tunnel excavations vary between 2 and 9 m. The very low seismic velocities away from the tunnel wall in two regions are associated with alcoves or 'cubbies' involving offsets in the wall of up to 10 m. The large variations in seismic velocity resolved over distances less than 15 m with signals of wavelength around 6–9 m are attributed largely to variations in the sizes and concentrations of fracture systems and cracks, though variations in the composition of the dolomite and the degree of water saturation in cracks and voids may also be important contributors to the velocity variations. The results also suggest that seismic velocity variations from reflection surveys may assist the interpretation of modelling studies of the stress regime in deep mines.

Acknowledgements

References

Bolt, B.A., 1978. Summary value smoothing with unequal intervals. J. Comput. Phys. 29, 357–360.

Crampin, S., 1981. A review of wave motion in anisotropic and cracked elastic media. Wave Motion 3, 343–391.

De Armorim, W.N., Hubral, P., Tygel, M., 1987. Computing field statics with the help of seismic tomography. Geophys. Prospect. 35, 907–917.

Hagedoorn, J.G., 1959. The plus–minus method of seismic refraction measurements. Geophys. Prospect. 7, 158–182.

Hampson, D., Russell, B., 1984. First-break interpretation using linear inversion. J. Can. Soc. Explor. Geophys. 20, 540–554.

Hawkins, L.R., 1961. The reciprocal method of routine shallow seismic refraction measurements. Geophysics 26, 806–819.

Hawkins, L.R., Whiteley, R.J., 1981. Shallow seismic refraction survey of the Woodlawn orebody. In: Whiteley, R.J. (Ed.), Geophysical Case Study of the Woodlawn Orebody, New South Wales, Australia. Pergamon, Oxford, pp. 497–506.

Henyey, T.H., Pomphrey, R.J., 1982. Self-consistent moduli of a cracked solid. Geophys. Res. Lett. 9, 903–906.

Hudson, J.A., 1981. Wave speeds and attenuation of elastic waves in material containing cracks. Geophys. J. R. Astron. Soc. 64, 133–150.

Jeffreys, H., 1937. On the smoothing of observed data. Proc. Cambridge Philos. Soc. 33, 444–450.

Kleyn, A.H., 1983. Seismic Reflection Interpretation. Applied Science Publ., London, 269 pp.

Leslie, I. (1995). A comparison of the methods of engineering seismic refraction analysis and generalized linear inversion for deriving statics and bedrock velocities, MSc thesis, Memorial University of Newfoundland, St. John's, Canada.

Lines, L.R., Treitel, S., 1984. Tutorial: a review of least-squares inversion and its application to geophysical problems. Geophys. Prospect. 32, 159–186.

O'Connell, R.J., Budiansky, B., 1977. Viscoelastic properties of fluid-saturated cracked solids. J. Geophys. Res. 82, 5719–5735.

Palmer, D., 1981. An introduction to the generalized reciprocal method of seismic refraction interpretation. Geophysics 46, 1508–1518.

Palmer, D., 1990. The generalized reciprocal method — an integrated approach to shallow refraction seismology. Explor. Geophys. 21, 33–44.

Schmidt, G., 1959. Results of underground seismic reflection investigations in the Siderite District of the Siegerland. Geophys. Prospect. 7, 287–290.

Spencer, C., Thurlow, J.G., Wright, J.A., White, D., Carroll, P., Milkereit, B., Reed, L., 1993. A Vibroseis reflection survey at the Buchans mine in central Newfoundland. Geophysics 58, 154–166.

Van Deventer, J.L., Eriksson, P.G., Snyman, C.P., 1986. The Thabazimbi iron ore deposits, north-west Transvaal. In: Anhaeusser, C., Maske, S. (Eds.), Mineral Deposits of Southern Africa vol. 1 Geological Society of South Africa, pp. 923–929.

Wright, C., 1996. Faulting and overburden and bedrock seismic velocities at Buchans and Gullbridge, Newfoundland, from seismic refraction measurements: applications to shallow geology and exploration. Can. J. Earth Sci. 33, 1201–1212.

Wright, C., 1999a. The LSDARC method of shallow seismic refraction interpretation. Eur. J. Environ. Eng. Geophys.

Wright, C., 1999b. Errors in timing of seismic sources in small-scale reflection and refraction surveys: a least-squares method for making corrections. Eur. J. Environ. Eng. Geophys.

Wright, C., Wright, J.A., Hall, J., 1994. Seismic reflection techniques for base metal exploration in eastern Canada: examples from Buchans, Newfoundland. J. Appl. Geophys. 32, 105–116.